TRANSMISSION COEFFICIENT FOR MULTI-LAYERED STRUCTURES AT ARBITRARY INCIDENT ANGLE

P. Zhang and M. L. Peterson
Mechanical Engineering Department
Fort Collins CO 80523

INTRODUCTION

Widespread adoption of process inspection is dependent on reduction of cost. In many applications the part geometry may not be known or may be sufficiently complex that it would be desirable to not follow all of the part contours. Fortunately, in cases where refraction of the wave between the coupling fluid and the part is low, relatively complex parts may be scanned without precisely following the part contours. This paper explores a problem where a complex part is scanned with a limited number of degrees of freedom in the scanning system. The close acoustic impedance match between the rubber part and the water coupling fluid allows this to be done efficiently. However, the refraction and attenuation of the wave in the material is still sufficiently high that it may be necessary to correct the amplitude of the received signal to account for the part geometry. Matrix propagator methods are used to create a model which will allow the effect of amplitude variation on the received signal to be explored for the curved specimen. The magnitude of the received signal will be adjusted to be equivalent to a normally incident wave.

The system which motivates this work is shown in Figure 1. In order to reduce the number of axes required to scan the tire section, four paintbrush transducers are used as transmitters. Four standard small diameter transducers are mounted in a scanning head and used as receivers. The entire sample can be scanned with two axes of motion as shown. However, the incident wave is not normal to the surface of the sample and may be as much as 20 degrees from normal. Detection of disbonds and material property changes at different locations on the sample must be obtained. The sample is modeled as five layers of a linear visco-elastic solid with measured or calculated materials properties.

The study of the transmission coefficient through multi-layered visco-elastic medium at arbitrary angles will provide the needed results to assess the sensitivity of the scanning method to known defects in a particular location. In addition knowledge of the acoustical properties of multi-layered structures is the basis for solving the inverse problem for unknown defects and the classification of defects.

Results in this paper are based on a linear visco-elastic model using properties of rubber. The transmission coefficient is found from matrix propagation methods which demonstrate numerical limitations. However, at the low frequencies and angles which are

Review of Progress in Quantitative Nondestructive Evaluation, Vol. 18
Edited by Thompson and Chimenti, Kluwer Academic/Plenum Publishers, 1999

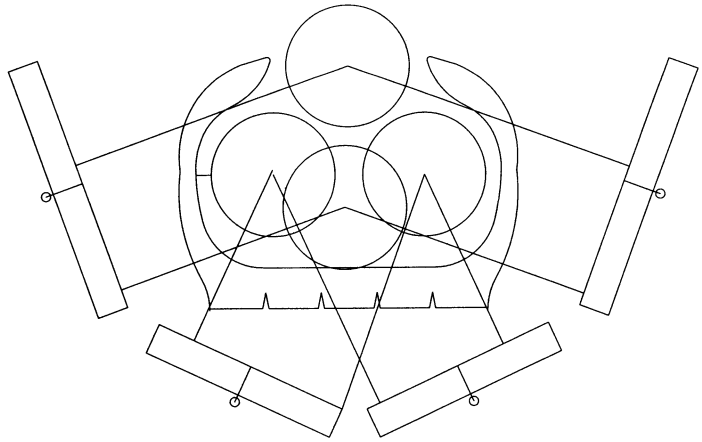

Figure 1. Configuration of transducers for tire inspection system.

near normal incidence the numerical problems are limited. Calculation results are then shown for the sensitivity of transmission coefficient to misalignment of the transducer and the sample seen in figure 1. Two cases are considered for sensitivity at a range of angles. First, the detection of one layer of unvulcanized material is considered. This is a situation which can occur under certain conditions in aircraft tires when landing on a wet surface. The damage to the surface of the tire is referred to as reversion. The second case is a disbond between layers of the composite. In both cases the transmission coefficient at the range of angles encountered will be compared to the undamaged composite.

THEORY

The model will employ a linear visco-elastic description of the material. Rubbers are typically described as being a linear visco-elastic materials [1,2,3,4]. Rubber exhibits internal damping and the stiffness increases as the frequency of loading is increased. Two simple models are commonly used to describe the response of rubber: a 2-element Voigt model and a 3-element model.

The simplest model used for linear viscoelasticity is the Voigt model (Figure 2). The complex Lame' constants are expressed as [4]:

$$\lambda^* = \frac{1}{3}(Y_v - Y_s),\ \mu^* = \frac{1}{2}Y_S \tag{1}$$

where Y_s and Y_v are the derivatoric and dilatational complex modulus, respectively. $Y_v = 3k$ and $Y_S = 2(\mu + \eta D)$, where μ is the elastic coefficient, η is the viscosity coefficient, D is a time derivative and k is the bulk modulus.

The Lame' constants can be rewritten:

$$\lambda^* = \lambda - \frac{2}{3}\eta D,\ \mu^* = \mu + \eta D \tag{2}$$

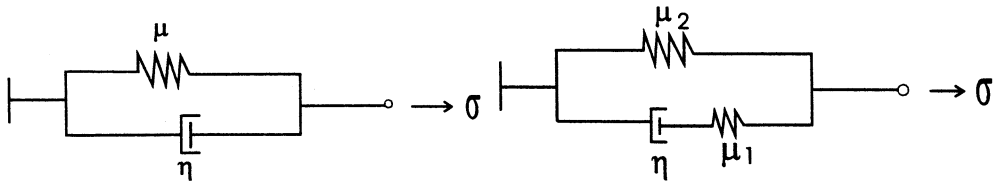

Figure 2. Rubber model (2-element Voigt model and 3-element mechanical model).

A slightly more complex model of rubber is the 3-element mechanical model, shown in figure 2. The 3-element model allows the stiffness of the rubber to be modeled as having a frequency dependence. This behavior more closely represents the actual behavior of real rubber materials. For 3-element model, as above, the constants are then:

$$\lambda^* = k - \frac{2}{3}\mu_2 - \frac{2}{3}\frac{\mu_1 \eta D}{\mu_1 + \eta D}, \quad \mu^* = \mu_2 + \frac{\mu_1 \eta D}{\mu_1 + \eta D} \tag{3}$$

For a plane harmonic incident wave, the complex modulus from the Voigt model have the form:

$$\lambda^* = \lambda + \frac{2}{3} i\omega\,\eta \ , \ \mu^* = \mu - i\omega\,\eta \tag{4}$$

where the real part of the complex modulus is the elastic modulus, while the imaginary part changes with frequency and the viscosity coefficient. For the 3-element mechanical model, the complex Lame' constants are similarly expressed, but the real parts and imaginary parts of the modulus simultaneously depend on the frequency and the viscosity coefficients.

For a plane incident wave the longitudinal wave (P wave) and vertically polarized shear wave (SV wave) are coupled. The horizontally polarized shear wave is independent from the P and SV wave. Only the SV and P wave will be considered and it will be assumed that u_t lies in the x-z plane and thus is independent of y. The vector potential in the solid is thus $\vec{\phi} = [0, \phi, 0]$. Therefore, in each solid layer j (the layers are from layer 2 to layer 6, the medium 1 and 7 are fluid water), the scalar and vector potentials of waves are [5]:

$$\varphi^{(j)} = \varphi_1^{(j)} \exp(i\alpha\,(z - z_{j-1})) + \varphi_2^{(j)} \exp(-i\alpha\,(z - z_{j-1})), \ z_j \le z \le z_{j-1} \tag{5}$$

$$\phi^{(j)} = \phi_1^{(j)} \exp(i\beta\,(z - z_{j-1})) + \phi_2^{(j)} \exp(-i\beta\,(z - z_{j-1})) \tag{6}$$

where $\alpha = k_l \cos\theta_l$, $\beta = k_t \cos\theta_t$, $\xi = k_i \sin\theta_i$. The $\exp(i\xi \cdot x - i\omega\, t)$ term is omitted, φ_1, φ_2 are the reflection amplitude and the incident amplitude for scalar potential, respectively, ϕ_1, ϕ_2 are the reflection amplitude and the incident amplitude for y-component of vector potential, respectively. Also, assume the vector potential $\vec{\varphi} = [\varphi_1, \varphi_2, \phi_1, \phi_2]^T$.

Boundary Conditions

For continuous boundary conditions, the stresses are continuous and the displacements are continuous at the interfaces between solids. If the displacement-stress vector is shown as: $\vec{f} = [u_1, u_3, \sigma_{33}, \sigma_{13}]^T$, then:

$$\vec{f}(z_j^+) = \vec{f}(z_j^-) \tag{7}$$

For the case of a 5-layer structure of rubber immersed in water, the shear stress vanishes for the interfaces between water and the solid. In addition the shear displacement is, in general, discontinuous. The scalar potential and vector potential then follow as:

$$\varphi^{(1)} = W \exp(-i\alpha\, z), \ \phi^{(1)} = 0 \tag{8a}$$

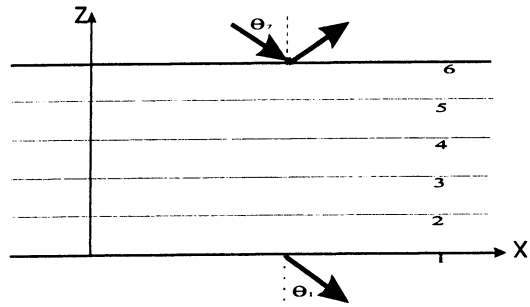

Figure 3. Five layers used in the model of the material. Layers two through six are solid rubber and medium 1 and 7 are fluid water. Angleθ - is the incident angle andθ $_{1}$ is the transmitted angle.

$$\varphi^{(6)} = \exp(-i\alpha\,(z - z_6)) + V\exp(i\alpha\,(z - z_6)),\ \phi^{(6)} = 0,\quad z \geq z_6 \tag{8b}$$

The particular case of a 5-layer structure of rubber with interlayer slip is also considered if the slip is between layer 4 and layer 5, the boundary conditions result in shear stresses which vanish at the interface and shear displacements are discontinuous. Normal stresses and displacements propagate through the interface, that is:

$$u_3^{(4-)} = u_3^{(4+)},\ \sigma_{33}^{(4-)} = \sigma_{33}^{(4+)} \tag{9}$$

Solution of Matrix Method

From equation of motion and Hookes' law, displacement and stress are obtained from the potentials, function as:

$$\vec{u} = (i\xi\varphi - \frac{\partial\phi}{\partial z}, 0, \frac{\partial\varphi}{\partial z} + i\xi\phi) \tag{10}$$

$$\vec{\sigma} = (-2\mu^{*}\xi(\gamma\phi - i\frac{\partial\varphi}{\partial z}), 0, 2\xi\mu^{*}(\gamma\varphi + i\frac{\partial\phi}{\partial z})) \tag{11}$$

the displacement-stress vector is related to potential vector as:

$$\vec{f} = [B(z, z_{j-1})]\vec{\varphi},\quad z_{j-1} \leq z \leq z_j \tag{12}$$

where, for every homogeneous layer, the potential vector$\vec{\varphi} = [\varphi_1, \varphi_2, \phi_1, \phi_2]^T$ is the same. Then, the displacement-stress vector from one layer to another layer is found to be:

$$\vec{f}(z_j) = [B(z_j, z_{j-1})][B(z_j - 1, z_{j-1})]^{-1}\vec{f}(z_{j-1}) \tag{13}$$

$[A^{(j)}] = [B(z_j, z_{j-1})][B(z_j - 1, z_{j-1})]^{-1}$, then for a continuous boundary condition, the displacement-stress vector is obtained from layer 2 to layer 6:

$$\vec{f}(z_6) = [A]\vec{f}(z_1) \tag{14}$$

where $[A]=[A^{(6)}][A^{(5)}][A^{(4)}][A^{(3)}][A^{(2)}]$, for every layer, the coefficients of matrix $A^{(J)}$ also are as in[5]. For the interfaces between a solid and a fluid, the displacement and stress matrix equation is:

$$\begin{bmatrix} u_1^{(6)} \\ u_3^{(6)} \\ \sigma_{33}^{(6)} \\ 0 \end{bmatrix} = [A] \begin{bmatrix} u_1^{(1)} \\ u_3^{(1)} \\ \sigma_{33}^{(1)} \\ 0 \end{bmatrix} \tag{15}$$

If the normal stress, the normal displacement and the boundary condition ($\sigma_{13}^{(6)}=0$), the equations of normal displacement and normal stress are derived:

$$u_3^{(6)} = M_{22}u_3^{(1)} + M_{23}\sigma_{33}^{(1)} \tag{16a}$$

$$\sigma_{33}^{(6)} = M_{32}u_3^{(1)} + M_{33}\sigma_{33}^{(1)} \tag{16b}$$

$$M_{ik} = A_{ik} - A_{i1}A_{4k} / A_{41} \tag{16c}$$

where A_{ik} are the coefficient of matrix $[A]$. Substituting equation (8) for the displacement and stress representations into equation (16), transmission coefficient is:

$$W = \frac{-2i\omega Z_1 \rho_1 \rho_7^{-1}}{M_{32} - i\omega Z_1 M_{33} - (M_{22} - i\omega Z_1 M_{23}) i\omega Z_7} \tag{17}$$

If interlayer slip occur between layer 4 and layer 5, the boundary conditions are discontinuous. However, a similar matrix method may be used to solve the problem. The displacement-stress vector from layer 2 to the top of layer 4 is expressed as:

$$\vec{f}(z_4^-) = [A^{(4)}]\vec{f}(z_3) \ , \ \vec{f}(z_4^-) = [A_1]\vec{f}(z_1) \tag{18}$$

where $[A_1]=[A^{(4)}][A^{(3)}][A^{(2)}]$, the coefficients in Matrix $[A^{(J)}]$ are the same as for continuous boundary conditions. The displacement-stress vectors in interface 1 and the top of layer 4 are similarly expressed in the form of equation (14). From normal displacement, normal stress and the boundary equation($\sigma_{13}^{(6)}=0$), normal displacement and normal stress matrix can be expressed:

$$\begin{bmatrix} u_3^{(4-)} \\ \sigma_{33}^{(4-)} \end{bmatrix} = [M_1] \begin{bmatrix} u_3^{(1)} \\ \sigma_{33}^{(1)} \end{bmatrix} \tag{19}$$

where $M_{1ik} = A_{1ik} - A_{1i1}A_{14k} / A_{141}$ is the coefficient of matrix $[M_1]$, A_{1ik} is the coefficient of matrix $[A_1]$. Also, displacement-stress vector from the bottom of layer 5 to layer 6 can be written $\vec{f}(z_6) = [A^{(6)}]\vec{f}(z_5)$, then:

$$\vec{f}(z_6) = [A_2]\vec{f}(z_4^+) \tag{20}$$

where $[A_2]=[A^{(6)}][A^{(5)}]$. Representations of displacement-stress vector for a slip boundary

conditions are similarly equation (16), then, normal displacement and normal stress matrix is given by:

$$\begin{bmatrix} u_3^{(6)} \\ \sigma_{33}^{(6)} \end{bmatrix} = [M_2] \begin{bmatrix} u_3^{(4+)} \\ \sigma_{33}^{(4+)} \end{bmatrix} \tag{21}$$

where $M_{2ik} = A_{2ik} - A_{2i1}A_{24k} / A_{241}$ are the coefficient of matrix $[M_2]$, A_{2ik} are the coefficient of matrix $[A_2]$. Substituting equation (9) and (19) into the matrix equation (21), a matrix representation of displacement and stress is found as

$$\begin{bmatrix} u_3^{(6)} \\ \sigma_{33}^{(6)} \end{bmatrix} = [M_s] \begin{bmatrix} u_3^{(1)} \\ \sigma_{33}^{(1)} \end{bmatrix} \tag{22}$$

where $[M_s] = [M_1][M_2]$. The result is similar to the result for a multi-layer structure immersed in water with continuous solid boundary conditions. By substituting equation (8) into equation (22), an expression for the transmission coefficient and reflection coefficient with interlayer slip between solid layers is obtained. The solution is the same as equation (17), but the matrix coefficients are different in the two cases.

NUMERICAL CALCULATIONS

Material Data

Calculations are shown for the Voigt material model for the case of the 5-layer system with both continuous and interlayer slip. The input data is shown in table 1. Material properties are based on measurements unless noted. The attenuation is extrapolated from published data [1] assuming a linear dependence of attenuation on frequency. For the case of reversion of the tread rubber (layer 2) material properties of soft (unvulcanized) rubber is used [6].

Calculation Results

Result for the transmission coefficient with continuous boundary conditions and interlayer slip are shown in figure 4. These figures show the dependence of the transmission coefficient on both frequency and angle of the incident wave. The plots of attenuation for different angles at a range of frequencies shows the importance of correction for misalignment as well as the altered sensitivity to these two types of defects at some incident angles. The slip boundary condition shown is, however, only an approximation to the boundary conditions in a disbond between belts. However, the type of variation of sensitivity encountered may be representative.

A comparison of the sensitivity of the continuous boundary conditions, interlayer slip in solids and reversion layer with angle is shown in figure 5. This figures show the three cases at 500 kHz, the nominal center frequency of the transducer used in the system. Additionally figures show the same sensitivity to angle at 300 kHz and 700kHz from the central frequency which corresponds to the 3 dB bandwidth of the transducer.

Table 1. Input data for 5-layer structures of rubber.

	Thickness (mm)	Velocity (m/s) (L and SV wave[1])		Attenuation (Nep) (L, S) [1]		Density (g/cm3)
Layer 2	15	1648 (L)	787 (S)	0.02	0.07	1.16
Layer 2 Unvulcanized	15	1480	706	0.02	0.07	0. 9
Layer 3	2	1639	782	0.02	0.07	1. 5
Layer 4	2	2413	1150	0.03	0.10	1. 6
Layer 5	2	2783	1326	0.03	0.12	1. 6
Layer 6	7	2164	1030	0.03	0.09	1. 5

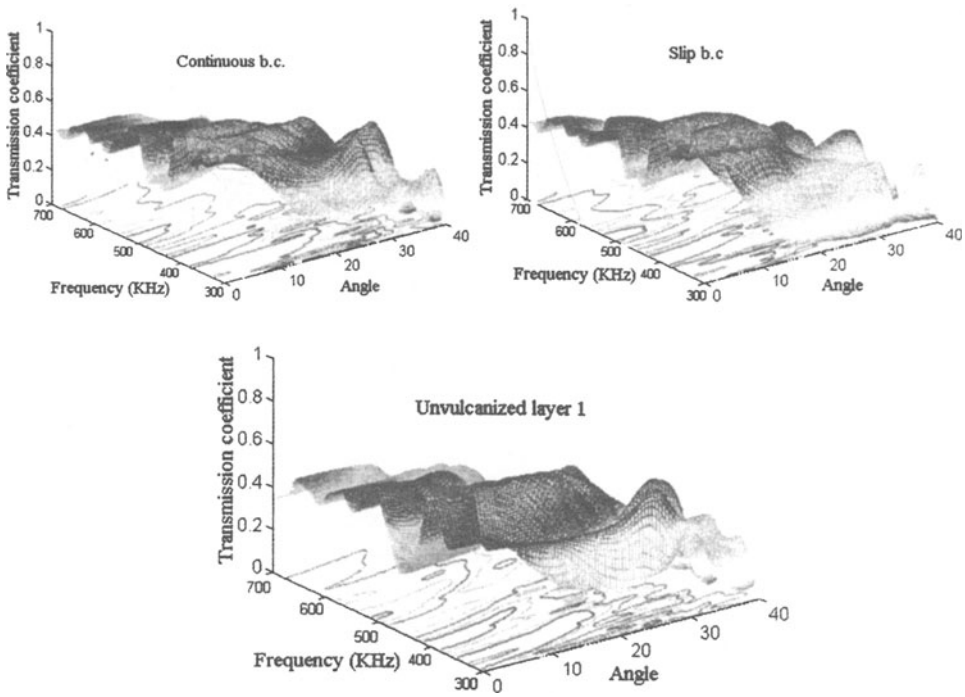

Figure 4. Transmission coefficient for continuous boundary conditions (left figure), interlayer slip between layer 4 and 5 in the solid (right) and for reversion of the tread (bottom).

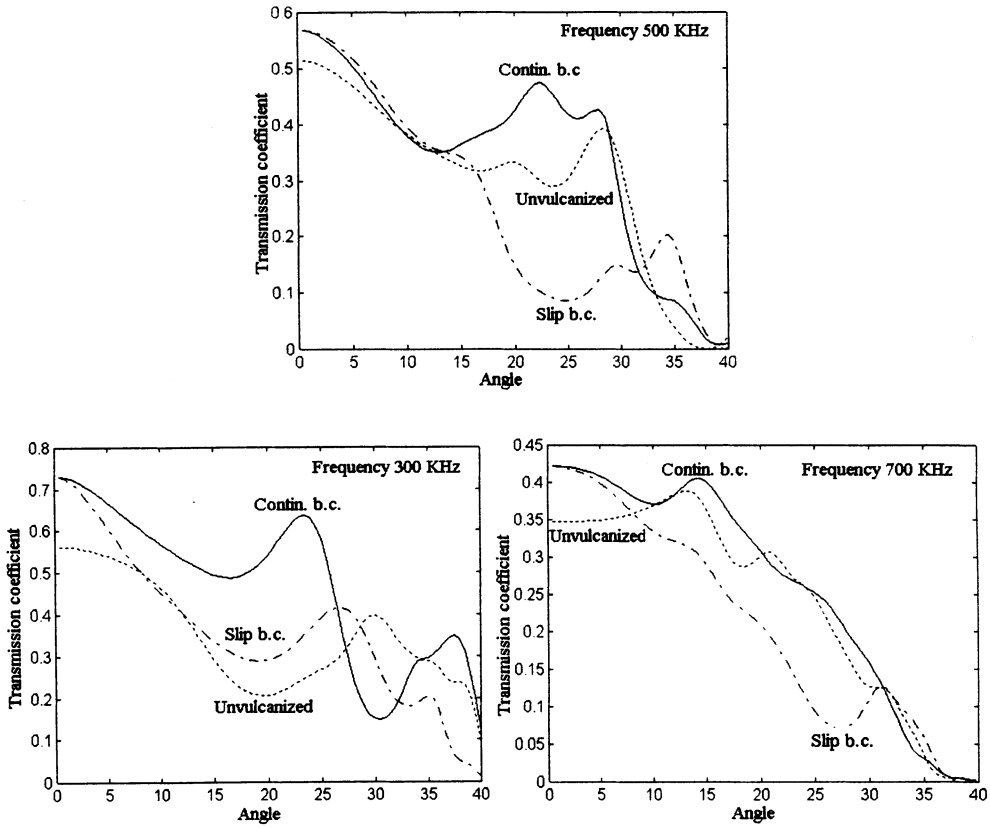

Figure 5. Transmission coefficients versus angles at different frequencies.

It is evident from these figures that the impact of the misalignment of the transducers in the orientation show in figure 1 cannot be neglected. What remains to be demonstrated is if the calculations shown are of sufficient accuracy given the uncertainty in the material properties as well as the incident angle, to be used to correct the received signal.

REFERENCES

1. A. W. Nolle and P. W. Sieck, J. Appl. Phys. 23(8), 888-894 (Aug.1952).
2. R. H. Nichols, J. Acoust. Soc. Am. 54(6),1763-1768, (1973).
3. J. C. Snowdon, *Vibration and Shock in Damped Mechanical Systems* (John Wiley & Sons, New York, 1968).
4. N. W. Tschoegl, *The Phenomenological Theory of Linear Viscoelastic Behavior* (Springer-Verlag, New York, 1989).
5. L. M. Brekhovskikh and O.A. Godin, *Acoustics of Layered Media I* (Springer-Verlag, New York, 1990).
6. J. Krautkramer and H. Krautkramer, *Ultrasonic Testing of Materials*, 3rd (Springer-Verlag, New York, 1983).